ACS OMEGA

Open Access

http://pubs.acs.org/journal/acsodf

Article

Theoretical Photoelectron Spectroscopy of Quadruple-Bonded Dimolybdenum(II,II) and Ditungsten(II,II) Paddlewheel Complexes: Performance of Common Density Functional Theory Methods

Abhik Ghosh* and Jeanet Conradie*

Cite This: *ACS Omega* 2024, 9, 12237−12241

Read Online

ACCESS | Metrics & More | Article Recommendations | Supporting Information

ABSTRACT: We have revisited the gas-phase photoelectron spectra of quadruple-bonded dimolybdenum(II,II) and ditungsten(II,II) paddlewheel complexes with modern density functional theory methods and obtained valuable calibration of four well-known exchange−correlation functionals, namely, BP86, OLYP, B3LYP*, and B3LYP. All four functionals were found to perform comparably, with discrepancies between calculated and experimental ionization potentials ranging from <0.1 to ∼0.5 eV, with the lowest errors observed for the classic pure functional BP86. All four functionals were found to reproduce *differences* in ionization potentials (IPs) between analogous Mo_2 and W_2 complexes, as well as large, experimentally observed ligand field effects on the IPs, with near-quantitative accuracy. The calculations help us interpret a number of differences between analogous Mo_2 and W_2 complexes through the lens of relativistic effects. Thus, relativity results in not only significantly lower IPs for the W_2 complexes but also smaller HOMO−LUMO gaps and different triplet states relative to their Mo_2 counterparts.

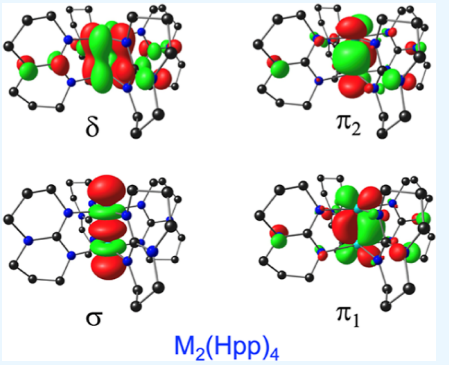

INTRODUCTION

Conceptualized by Cotton nearly 60 years ago,[1−3] metal−metal quadruple bonds are an icon of inorganic chemistry.[4] They vary remarkably in terms of their electronic properties such as ionization potentials (IPs), electron affinities, redox potentials, the nature of the frontier orbitals, HOMO−LUMO gaps, and singlet−triplet gaps.[4−6] The critical gas-phase photoelectron spectroscopy (PES) measurements,[7−14] however, were made largely in the latter half of the last century and still remain inadequately explored with modern density functional theory (DFT) methods.[13−15] We recently made an effort to close this knowledge gap with a comparative DFT study of quadruple-bonded metalloporphyrin[16] and metallocorrole[17] dimers.[18] Here, we have extended these studies to *nonporphyrinoid* dimolybdenum(II,II) and ditungsten(II,II) paddlewheel complexes. We have examined three series of compounds—$M_2(OFm)_4$, $M_2(Me_2Fa)_4$, and $M_2(Hpp)_4$—and compared the results with those for $M_2(Por)_2$, where OFm = formate, Me_2Fa = *N*,*N*′-dimethylformamidinate, Hpp = hexahydropyrimidinopyrimidine, Por = unsubstituted porphyrin dianion, and M = Mo and W (Scheme 1). The results afford not only valuable calibration of the performance of common exchange−correlation functionals but also insights into periodic trends and relativistic effects as they pertain to metal−metal quadruple bonds. For transition metals, the two key scalar relativistic effects (as distinguished from spin−orbit coupling effects) are a stabilization of s orbitals and a destabilization of d orbitals. For a broader introduction to the subject, the reader may consult

Scheme 1. Quadruple-Bonded Compounds Studied in This Work

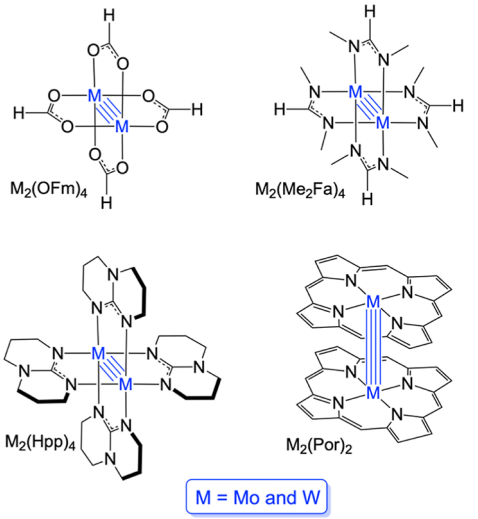

Received: January 8, 2024
Revised: February 13, 2024
Accepted: February 22, 2024
Published: March 4, 2024

https://doi.org/10.1021/acsomega.4c00269
ACS Omega 2024, 9, 12237−12241

Table 1. Calculated and Experimental IPs (eV) for the Molecules Studied[a,b]

	BP86-D3		OLYP-D3		B3LYP*-D3		B3LYP-D3		PES
	IP_v	IP_a	IP_v	IP_a	IP_v	IP_a	IP_v	IP_a	
$Mo_2(OFm)_4$ (D_{4h})	7.44	7.38	7.19	7.12	7.23	7.16	7.21	7.12	7.5[c]
$W_2(OFm)_4$ (D_{4h})	6.93	6.91	6.59	6.56	6.64	6.62	6.58	6.55	
$Mo_2(Me_2Fa)_4$ (D_{4h})	5.36	5.30	5.10	5.04	5.11	5.04	5.08	4.99	5.63[d]
$W_2(Me_2Fa)_4$ (D_{4h})	5.00	4.95	4.71	4.65	4.71	4.65	4.65	4.59	5.23[d]
$Mo_2(Hpp)_4$ (D_4)	3.82	3.71	3.61	3.49	3.70	3.56	3.69	3.53	4.33 (4.01)[e]
$W_2(Hpp)_4$ (D_4)	3.41	3.31	3.13	3.03	3.19	3.08	3.23	3.11	3.76 (3.51)[e]
{Mo[Por]}$_2$ (D_{4h})	5.72	5.67	5.39	5.38	5.39		5.33	5.23	
{W[Por]}$_2$ (D_{4h})	5.21		4.83	4.82	4.85		4.78		

[a]The calculations were carried out with a scalar-relativistic ZORA (zeroth order regular approximation to the Dirac equation)[34] Hamiltonian, all-electron ZORA STO-TZ2P basis sets, fine integration grids and tight criteria for SCF and geometry optimization cycles, and appropriate point group symmetry, all as implemented in the ADF program system.[35] [b]The subscripts v and a indicate "vertical" and "adiabatic", respectively. [c]Ref 7. [d]Experimental measurements were carried out on *N*,*N*′-diphenylformamidinato (Ph_2Fa) complexes; ref 13. [e]The values within parentheses are the observed onset potentials; ref 14.

a nontechnical review article by Pyykkö[19] and a popular science account in *American Scientist* by one of us.[20] This study adds to our growing appreciation of relativistic effects in coordination chemistry.[21−25]

RESULTS AND DISCUSSION

Table 1 presents DFT-based IPs and electron affinities calculated with the ΔSCF method using different exchange−correlation functionals, namely, the classic pure functional BP86;[26,27] the pure functional OLYP,[28,29] which has often yielded improved results; and the hybrid functionals B3LYP[30] and B3LYP*,[31,32] with 20 and 15% Hartree−Fock exchange, respectively, all augmented with Grimme's D3 dispersion corrections.[33] Also listed in Table 1 are relevant experimental IPs, derived largely from gas-phase PES. Figure 1 presents a comparative MO energy level diagram for a selection of the compounds studied, namely, the two Hpp complexes and, for comparison, the two analogous porphyrin complexes.[18] Figure 2 depicts key metal-based OLYP-D3 frontier MOs for $Mo_2(Hpp)_4$ (the analogous MOs for the W_2 complex are visually exceedingly similar and, accordingly, not shown). The results lead to the following conclusions.

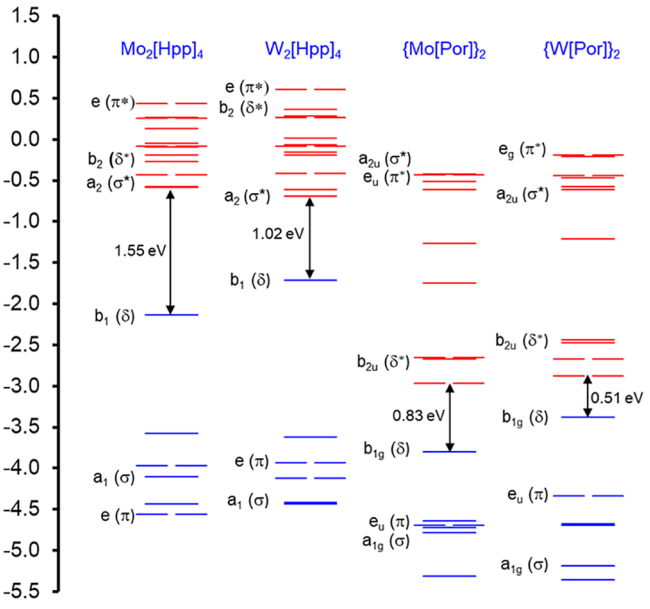

Figure 1. Comparative OLYP-D3/ZORA-STO-TZ2P MO energy level diagram (eV) for $M_2(Hpp)_2$ (D_4) and $M_2(Por)_2$ (D_{4h}), where M = Mo and W. Also indicated are MO irreps for the point group in question.

The present scalar-relativistic calculations with large Slater-type basis sets present some of the first *quantitative* insights (relative to early theoretical studies[10,13−15]) into the performance of DFT methods with respect to photoelectron spectra of classic metal−metal quadruple-bonded systems. Although we have long known that DFT methods do an impressive job of reproducing gas-phase IPs and electron affinities of organic and main-group systems (see selected studies from our laboratory[36−43]), the performance of DFT vis-à-vis transition-metal systems has been rather an open question. On the one hand, DFT methods have long struggled with reproducing the spin-state energetics of transition-metal complexes.[44−52] On the other hand, DFT has an excellent track record of correctly predicting the redox site in metalloporphyrin-type complexes, such as nickel hydroporphyrins[53] and a number of metal−metal multiple-bonded metallocorrole dimers.[54] To our satisfaction, for $Mo_2(OFm)_4$, all four exchange−correlation functionals yielded vertical IPs in semiquantitative agreement with gas-phase PES, with the best agreement observed for BP86-D3. On the other hand, the calculated vertical IPs of the Hpp complexes are lower than the corresponding experimental values by ∼0.5 eV; interestingly, the errors relative to experimental "onset potentials" are much lower, only about 0.1−0.2 eV. We view these as rather modest errors that we can easily "live with". More importantly, the calculations reproduce differences in IPs within pairs of analogous Mo_2 and W_2 complexes with near-quantitative accuracy. Overall, the four functionals examined appear to perform comparably, with the classic pure functional BP86 exhibiting the best agreement with gas-phase PES.

Experimentally, the first IPs span a > 4 eV range for dimolybdenum(II,II) paddlewheel complexes, from 4.33 eV for $Mo_2(Hpp)_4$14 to 8.76 eV for $Mo_2(CF_3COO)_4$.11 For the analogous ditungsten(II,II) complexes, the IPs span a slightly smaller range of 3.63 eV, from 3.76 eV for $W_2(Hpp)_4$14 to 7.39 eV for $W_2(CF_3COO)_4$.[11] The calculations, regardless of the functional, appear to do an excellent job of reproducing the large ligand field effects on the experimentally observed IPs. The reason underlying the large ligand field effects seems rather obvious: in each case, the HOMO corresponds to the δ bond (see Figures 1 and 2), which is exclusively localized on the

https://doi.org/10.1021/acsomega.4c00269
ACS Omega 2024, 9, 12237−12241

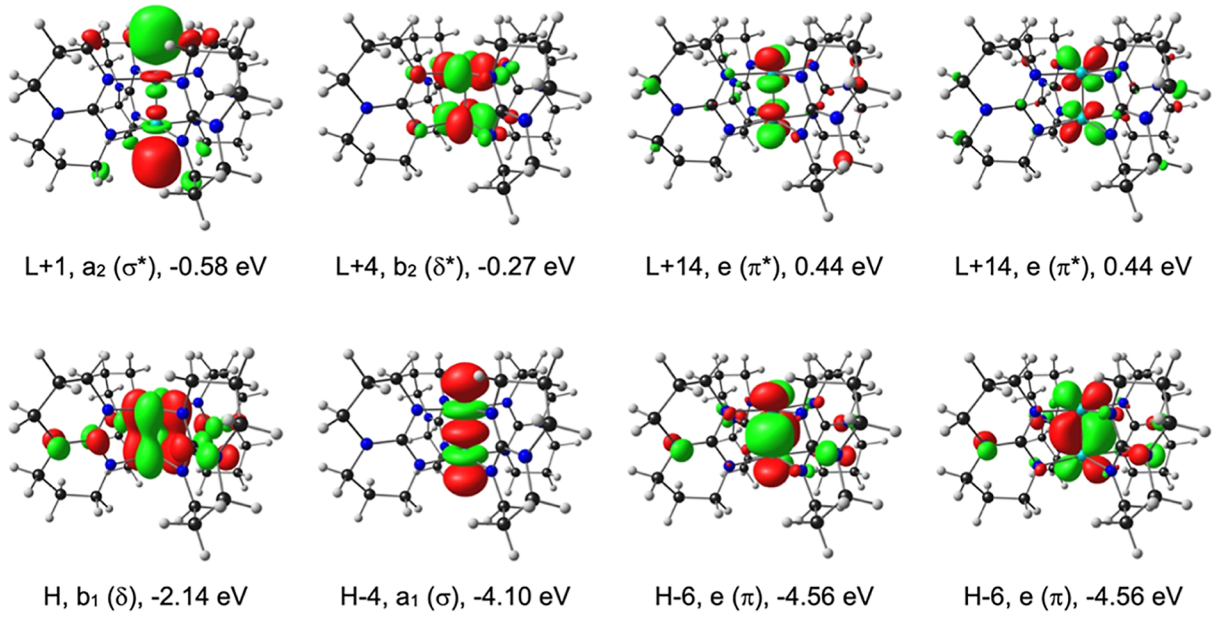

Figure 2. Selected OLYP-D3/ZORA-STO-TZ2P frontier MOs for $Mo_2(Hpp)_2$. H and L refer to HOMO and LUMO, respectively. Also shown are D_4 irreps and Kohn−Sham orbital energies (eV).

bimetal unit and, accordingly, highly susceptible to the ligands' electronic effects.

Both calculated and experimental data reveal systematic differences between the IPs of analogous Mo_2 and W_2 complexes, with the vertical first IPs of the latter being lower by a margin of ∼0.5 eV (Table 1). Likewise, both Kohn−Sham orbital energy spectra and experimental PES measurements indicate that the same holds for metal−metal π-bonds.[13−15] Based on comparisons between scalar-relativistic and non-relativistic calculations with the same basis sets (as described in detail in earlier studies from our laboratory[21−24]), the differences in IPs between analogous Mo_2 and W_2 systems could be largely attributed to differences in relativistic effects for the two metals, with the W 5d orbitals significantly more destabilized by relativity than the Mo 4d orbitals. An interesting point is that the relativistic effects observed here are larger than, indeed almost twice, what we have observed for other analogous pairs of 4d and 5d element complexes.[21,24,25] A plausible explanation appears to be that our earlier studies involved mononuclear complexes, whereas here we are concerned with a bimetal unit with the MOs in question derived from overlapping d orbitals from *two* metal atoms.

In contrast to the above, Figure 1 shows that metal−metal σ and σ^* orbitals exhibit slightly *lower* orbital energies in W_2 complexes than those in their Mo_2 counterparts. This stabilization reflects the significant admixture of metal s character in these orbitals and the fact that the W 6s orbital is significantly more relativistically stabilized than the Mo 5s orbital.[19,20] The relativistic destabilization of the δ^* HOMO and the stabilization of the σ^* LUMO/LUMO+1 in the W_2 complexes relative to their Mo_2 counterparts translate to significantly smaller HOMO−LUMO gaps for the former (Figure 1). Interestingly, as noted earlier,[18] the LUMOs of the porphyrin complexes consist of a degenerate pair of porphyrin-based orbitals, which results in both exceedingly low HOMO−LUMO gaps and large electron affinities relative to the nonporphyrin complexes. In fact, according to our calculations, a positive EA is not predicted for any of the nonporphyrin-supporting ligands, except for small values < 0.5 eV for carboxylate-supporting ligands.

The scalar-relativistic calculations presented here predict different triplet states for Mo_2 and W_2 paddlewheel complexes. Taking the Hpp complexes as our paradigm, B3LYP*-D3 calculations on $Mo_2(Hpp)_4$ predict a $\delta^1\delta^{*1}$ triplet state at 1.09 eV and a $\delta^1\sigma^{*1}$ state at 1.49 eV above the ground singlet state (both values refer to adiabatic energies). For $W_2(Hpp)_4$, in contrast, our calculations predict a lower-energy $\delta^1\sigma^{*1}$ triplet state at 0.89 eV and a higher-energy $\delta^1\delta^{*1}$ triplet state at 1.45 eV, an interesting example of a relativity-driven reversal of excited-state energetics (see refs 5 and 6 for a general background).

CONCLUSIONS

In summary, revisiting the gas-phase photoelectron spectra of quadruple-bonded dimolybdenum(II,II) and ditungsten(II,II) complexes with modern DFT methods has yielded a valuable calibration of four popular exchange−correlation functionals. In spite of a possible systematic error of a few tenths of an eV in the absolute values of the IPs, the functionals examined reproduce differences in IPs between analogous Mo_2 and W_2 complexes and large ligand field effects with near-quantitative accuracy. The calculations help us interpret a number of electronic differences between analogous Mo_2 and W_2 complexes in terms of differential relativistic effects. Thus, relativity results in not only lower IPs for the W_2 complexes but also smaller HOMO−LUMO gaps and different triplet states relative to their Mo_2 counterparts.

ASSOCIATED CONTENT

Supporting Information

The Supporting Information is available free of charge at https://pubs.acs.org/doi/10.1021/acsomega.4c00269.

Optimized DFT coordinates (PDF)

https://doi.org/10.1021/acsomega.4c00269
ACS Omega 2024, 9, 12237−12241

AUTHOR INFORMATION

Corresponding Authors

Abhik Ghosh − *Department of Chemistry, UiT − the Arctic University of Norway, N-9037 Tromsø, Norway;* orcid.org/0000-0003-1161-6364; Email: abhik.ghosh@uit.no

Jeanet Conradie − *Department of Chemistry, UiT − the Arctic University of Norway, N-9037 Tromsø, Norway; Department of Chemistry, University of the Free State, Bloemfontein 9300, Republic of South Africa;* orcid.org/0000-0002-8120-6830; Email: conradj@ufs.ac.za

Complete contact information is available at: https://pubs.acs.org/10.1021/acsomega.4c00269

Notes

The authors declare no competing financial interest.

ACKNOWLEDGMENTS

This work was supported by grant no. 324139 of the Research Council of Norway (A.G.) and grant nos. 129270 and 132504 of the South African National Research Foundation (J.C.).

REFERENCES

(1) Cotton, F. A.; Harris, C. B. The Crystal and Molecular Structure of Dipotassium Octachlorodirhenate(III) Dihydrate, $K_2[Re_2Cl_8]$. 2H2O. *Inorg. Chem.* **1965**, *4* (3), 330−333.

(2) Cotton, F. A. Metal-Metal Bonding in $[Re_2X_8]^{2-}$ Ions and Other Metal Atom Clusters. *Inorg. Chem.* **1965**, *4*, 334−336.

(3) Cotton, F. A. Discovering and Understanding Multiple Metal-to-Metal bonds. *Acc. Chem. Res.* **1978**, *11*, 225−232.

(4) Cotton, F. A., Murillo, C. A., Walton, R. A., Eds. In *Multiple bonds between metal atoms*; Springer: New York, 2005, p 818.

(5) Trogler, W. C.; Gray, H. B. Electronic Spectra and Photochemistry of Complexes Containing Quadruple Metal-Metal Bonds. *Acc. Chem. Res.* **1978**, *11*, 232−239.

(6) Cotton, F. A.; Nocera, D. G. The whole story of the two-electron bond, with the δ bond as a paradigm. *Acc. Chem. Res.* **2000**, *33*, 483−490.

(7) Green, J. C.; Hayes, A. J. Ionization energies of an Mo−Mo quadruple bond; a He(I) photoelectron study of some molybdenum-dicarboxylate dimers. *Chem. Phys. Lett.* **1975**, *31*, 306−307.

(8) Bursten, B. E.; Cotton, F. A.; Cowley, A. H.; Hanson, B. E.; Lattman, M.; Stanley, G. G. Strong metal-to-metal quadruple bonds in a series of five isostructural compounds as indicated by photoelectron spectroscopy. *J. Am. Chem. Soc.* **1979**, *101*, 6244−6249.

(9) Garner, C. D.; Hillier, I. H.; MacDowell, A. A.; Walton, I. B.; Guest, M. F. Nature of Cr—Cr "quadruple bond". Photoelectron spectra of solid tetra-μ-acetatodichromium(II), solid and gaseous tetra-μ-trifluoroacetate-dichromium(II), and gaseous tetra-μ-{6-methyl-2-hydroxypyridine}-dichromium(II) and -dimolybdenum(II). *J. Chem. Soc., Faraday Trans. II* **1979**, *75*, 485−493.

(10) Cotton, F. A.; Hubbard, J. L.; Lichtenberger, D. L.; Shim, I. Comparative studies of molybdenum-molybdenum and tungsten-tungsten quadruple bonds by SCF-X.alpha.-SW calculations and photoelectron spectroscopy. *J. Am. Chem. Soc.* **1982**, *104*, 679−686.

(11) Bancroft, G. M.; Pellach, E.; Sattelberger, A. P.; McLaughlin, K. W. The photoelectron spectrum of quadruply bonded $W_2(O_2CCF_3)4$. *J. Chem. Soc., Chem. Commun.* **1982**, 752−754.

(12) Lichtenberger, D. L.; Ray, C. D.; Stepniak, F.; Chen, Y.; Weaver, J. H. The electronic nature of the metal-metal quadruple bond: Variable photon energy photoelectron spectroscopy of $Mo_2(O_2CCH_3)_4$. *J. Am. Chem. Soc.* **1992**, *114*, 10492−10497.

(13) Lichtenberger, D. L.; Lynn, M. A.; Chisholm, M. H. Quadruple Metal− Metal Bonds with Strong Donor Ligands. Ultraviolet Photoelectron Spectroscopy of $M_2(form)_4$ (M= Cr, Mo, W; form = N,Ń-diphenylformamidinate). *J. Am. Chem. Soc.* **1999**, *121*, 12167−12176.

(14) Cotton, F. A.; Gruhn, N. E.; Gu, J.; Huang, P.; Lichtenberger, D. L.; Murillo, C. A.; Van Dorn, L. O.; Wilkinson, C. C. Closed-Shell Molecules That Ionize More Readily Than Cesium. *Science* **2002**, *298*, 1971−1974.

(15) Ziegler, T. Theoretical study on the quadruple metal bond in d^4-d^4 binuclear tetracarboxylate complexes of chromium, molybdenum, and tungsten by the Hartree-Fock-Slater transition-state method. *J. Am. Chem. Soc.* **1985**, *107*, 4453−4459.

(16) Collman, J. P.; Arnold, H. J. Multiple Metal-Metal Bonds in 4d and 5d Metal-Porphyrin Dimers. *Acc. Chem. Res.* **1993**, *26*, 586−592.

(17) Alemayehu, A. B.; Mcormick-Mpherson, L. J.; Conradie, J.; Ghosh, A. Rhenium Corrole Dimers: Electrochemical Insights into the Nature of the Metal−Metal Quadruple Bond. *Inorg. Chem.* **2021**, *60*, 8315−8321.

(18) Conradie, J.; Vazquez-Lima, H.; Alemayehu, A. B.; Ghosh, A. Comparing Isoelectronic, Quadruple-Bonded Metalloporphyrin and Metallocorrole Dimers: Scalar-Relativistic DFT Calculations Predict a ∼ 1 eV Range for Ionization Potential and Electron Affinity. *ACS Phys. Chem. Au* **2022**, *2*, 70−78.

(19) Pyykkö, P. Relativistic effects in chemistry: more common than you thought. *Annu. Rev. Phys. Chem.* **2012**, *63*, 45−64.

(20) For a popular account of relativistic effects in chemistry, see: Ghosh, A.; Ruud, K. Relativity and the World of Molecules. *Am. Sci.* **2023**, *111*, 160−167.

(21) Alemayehu, A. B.; Vazquez-Lima, H.; Gagnon, K. J.; Ghosh, A. Stepwise Deoxygenation of Nitrite as a Route to Two Families of Ruthenium Corroles: Group 8 Periodic Trends and Relativistic Effects. *Inorg. Chem.* **2017**, *56*, 5285−5294.

(22) Alemayehu, A. B.; Mcormick, L. J.; Vazquez-Lima, H.; Ghosh, A. Relativistic Effects on a Metal−Metal Bond: Osmium Corrole Dimers. *Inorg. Chem.* **2019**, *58*, 2798−2806.

(23) Alemayehu, A. B.; Vazquez-Lima, H.; McCormick, L. J.; Ghosh, A. Relativistic effects in metallocorroles: comparison of molybdenum and tungsten biscorroles. *Chem. Commun.* **2017**, *53*, 5830−5833.

(24) Demissie, T. B.; Conradie, J.; Vazquez-Lima, H.; Ruud, K.; Ghosh, A. Rare and Nonexistent Nitrosyls: Periodic Trends and Relativistic Effects in Ruthenium and Osmium Porphyrin-Based $\{MNO\}^7$ Complexes. *ACS Omega* **2018**, *3*, 10513−10516.

(25) Braband, H.; Benz, M.; Spingler, B.; Conradie, J.; Alberto, R.; Ghosh, A. Relativity as a Synthesis Design Principle: A Comparative Study of [3+ 2] Cycloaddition of Technetium(VII) and Rhenium(VII) Trioxo Complexes with Olefins. *Inorg. Chem.* **2021**, *60*, 11090−11097.

(26) Becke, A. D. J. Density functional calculations of molecular bond energies. *Chem. Phys.* **1986**, *84*, 4524−4529.

(27) Perdew, J. P. Density-functional approximation for the correlation energy of the inhomogeneous electron gas. *Phys. Rev. B* **1986**, *33*, 8822−8824.

(28) Handy, N. C.; Cohen, A. Left-Right Correlation Energy. *J. Mol. Phys.* **2001**, *99*, 403−412.

(29) Lee, C.; Yang, W. T.; Parr, R. G. Development of the Colle-Salvetti Correlation-Energy Formula into a Functional of the Electron-Density. *Phys. Rev. B* **1988**, *37*, 785−789.

(30) Stephens, P. J.; Devlin, F. J.; Chabalowski, C. F.; Frisch, M. J. Ab initio calculation of vibrational absorption and circular dichroism spectra using density functional force fields. *J. Phys. Chem.* **1994**, *98*, 11623−11627.

(31) Reiher, M.; Salomon, O.; Hess, B. A. Reparameterization of hybrid functionals based on energy differences of states of different multiplicity. *Theor. Chem. Acc.* **2001**, *107*, 48−55.

(32) Salomon, O.; Reiher, M.; Hess, B. A. Assertion and validation of the performance of the B3LYP* functional for the first transition metal row and the G2 test set. *J. Chem. Phys.* **2002**, *117*, 4729−4737.

(33) Ghosh, A.; Vangberg, T.; Gonzalez, E.; Taylor, P. Molecular structures and electron distributions of higher-valent iron and manganese porphyrins. Density functional theory calculations and some preliminary open-shell coupled-cluster results. *J. Porphyrins Phthalocyanines* **2001**, *05*, 345−356.

(34) Van Lenthe, E. V.; Snijders, J. G.; Baerends, E. J. The zero-order regular approximation for relativistic effects: The effect of spin−orbit coupling in closed shell molecules. *J. Chem. Phys.* **1996**, *105* (15), 6505−6516.
(35) Velde, G. T.; Bickelhaupt, F. M.; Baerends, E. J.; Guerra, C. F.; van Gisbergen, S. J. A.; Snijders, J. G.; Ziegler, T. Chemistry with ADF. *J. Comput. Chem.* **2001**, *22*, 931−967.
(36) Ghosh, A.; Almlöf, J. The ultraviolet photoelectron spectrum of free-base porphyrin revisited. The performance of local density functional theory. *Chem. Phys. Lett.* **1993**, *213*, 519−521.
(37) Ghosh, A. Substituent effects on valence ionization potentials of free base porphyrins: A local density functional study. *J. Am. Chem. Soc.* **1995**, *117*, 4691−4699.
(38) Ghosh, A.; Vangberg, T. Valence ionization potentials and cation radicals of prototype porphyrins. The remarkable performance of nonlocal density functional theory. *Theor. Chem. Acc.* **1997**, *97*, 143−149.
(39) Ghosh, A.; Conradie, J. Theoretical Photoelectron Spectroscopy of Low-Valent Carbon Species: A ∼ 6 eV Range of Ionization Potentials among Carbenes, Ylides, and Carbodiphosphoranes. *ACS Org. Inorg. Au* **2023**, *3*, 92−95.
(40) Ghosh, A.; Conradie, J. Twist-Bent Bonds Revisited: Adiabatic Ionization Potentials Demystify Enhanced Reactivity. *ACS Omega* **2022**, *7*, 37917−37921.
(41) Ghosh, A.; Conradie, J. The Perfluoro Cage Effect: A Search for Electron-Encapsulating Molecules. *ACS Omega* **2023**, *8*, 4972−4975.
(42) Ghosh, A.; Conradie, J. Porphyryne. *ACS Omega* **2022**, *7*, 40275−40278.
(43) Torstensen, K.; Ghosh, A. From Diaminosilylenes to Silapyramidanes: Making Sense of the Stability of Divalent Silicon Compounds. *ACS Org. Inorg. Au* **2024**, *4*, 102−105.
(44) Ghosh, A.; Taylor, P. R. High-level ab initio calculations on the energetics of low-lying spin states of biologically relevant transition metal complexes: a first progress report. *Curr. Opin. Chem. Biol.* **2003**, *7*, 113−124.
(45) Ghosh, A. Transition metal spin state energetics and non-innocent systems: challenges for DFT in the bioinorganic arena. *J. Biol. Inorg. Chem.* **2006**, *11*, 712−724.
(46) Conradie, J.; Ghosh, A. DFT calculations on the spin-crossover complex Fe (salen)(NO): A quest for the best functional. *J. Phys. Chem. B* **2007**, *111*, 12621−12624.
(47) Wasbotten, I. H.; Ghosh, A. Spin-State Energetics and Spin-Crossover Behavior of Pseudotetrahedral Cobalt(III)−Imido Complexes. The Role of the Tripodal Supporting Ligand. *Inorg. Chem.* **2007**, *46*, 7890−7898.
(48) Ye, S.; Neese, F. Accurate modeling of spin-state energetics in spin-crossover systems with modern density functional theory. *Inorg. Chem.* **2010**, *49*, 772−774.
(49) Radon, M. Spin-state energetics of heme-related models from DFT and coupled cluster calculations. *J. Chem. Theory Comput.* **2014**, *10*, 2306−2321.
(50) Swart, M.; Gruden, M. Spinning around in transition-metal chemistry. *Acc. Chem. Res.* **2016**, *49*, 2690−2697.
(51) Roemelt, M.; Pantazis, D. A. Multireference approaches to spin-state energetics of transition metal complexes utilizing the density matrix renormalization group. *Adv. Theory Simul.* **2019**, *2*, 1800201.
(52) Phung, Q. M.; Nam, H. N.; Ghosh, A. Local Oxidation States in $\{FeNO\}^{6-8}$ Porphyrins: Insights from DMRG/CASSCF−CASPT2 Calculations. *Inorg. Chem.* **2023**, *62*, 20496−20505.
(53) Ryeng, H.; Gonzalez, E.; Ghosh, A. DFT at Its Best: Metal-versus Ligand-Centered Reduction in Nickel Hydroporphyrins. *J. Phys. Chem. B* **2008**, *112*, 15158−15173.
(54) Osterloh, W. R.; Conradie, J.; Alemayehu, A. B.; Ghosh, A.; Kadish, K. M. The Question of the Redox Site in Metal−Metal Multiple-Bonded Metallocorrole Dimers. *ACS Org. Inorg. Au* **2023**, *3*, 35−40.

https://doi.org/10.1021/acsomega.4c00269
ACS Omega 2024, 9, 12237−12241